Asian Journal of Chemistry; Vol. 37, No. 11 (2025), 2831-2838
ASIAN JOURNAL OF CHEMISTRY
https://doi.org/10.14233/ajchem.2025.34214

Synthesis, Characterization, DFT Calculation and Evaluation of Antimicrobial, Antioxidant and Anticancer Properties of Cadmium(II) Complex of N-[2-Hydroxy-3-methylbenzyl]valine

MOHD SHAHZAD[1,*], NAMAN CHAUDHARY and SHASTI BALLABH MISHRA

Department of Chemistry, Motiram Baburam Government Post Graduate College, Haldwani-263139, India

*Corresponding authors: E-mail: mshahzad10594@gmail.com

Received: 15 June 2025 *Accepted*: 6 October 2025 *Published online*: 27 October 2025 AJC-22173

In this work, a novel cadmium(II) complex was synthesized through a complexation reaction between cadmium acetate and a ligand obtained through nucleophilic substitution. The structural and electronic properties were examined by IR, NMR, UV-Vis spectroscopy, SEM, PXRD and DFT calculation techniques. FT-IR validated the metal-ligand coordination, whereas UV-Vis spectra revealed electronic changes and metal-to-ligand charge transfer (MLCT) during cadmium complexation. SEM demonstrated morphological alterations, with the complex displaying a dense and stable architecture. XRD study indicated a transition from a monoclinic (*P*21/*a*) crystal system in the ligand to a hexagonal (*P*63/*mmc*) system in the metal complex, implying structural reorganization. The biological activities of the ligand before and after coordination were evaluated and compared in terms of antimicrobial activity (against *Aspergillus niger* and *Escherichia coli*), antioxidant activity (using the DPPH radical scavenging assay), and anticancer activity (against MCF-7 breast cancer cells). In antimicrobial activity, Cd(II) complex demonstrated enhanced antifungal activity against *A. niger* while ligand has greater antibacterial efficacy against *E. coli*. Antioxidant activity of ligand exhibited superior radical scavenging at low concentration while Cd(II) complex approached the greater potency of ascorbic acid (standard) at higher doses. Anticancer properties evaluated the complex displayed the stronger anticancer effects than the ligand due to metal coordination with ligand.

Keywords: Valine, Cadmium(II) complex, Density functional theory, Biological activities.

INTRODUCTION

Many transitional metal complexes are used as a chemotherapeutic agent through its DNA-binding capabilities, antimicrobial activities and antioxidant properties [1-3]. Valine, an essential α-amino acid, and its 4*d*-transition metal complexes play vital roles in the biological systems and exhibit promising therapeutic potential [4,5]. Among these, silver(I) complex displayed exceptional antimicrobial activities, including strong activity against methicillin-resistant *Staphylococcus aureus* (MRSA) with a low MIC values [6]. Similarly, valine-based Ru(II) complex exhibits potent anticancer activity through ROS-mediated apoptosis against particular efficacy against MCF-7 breast cancer cells with an IC_{50} [7]. As a result of these valine-derived metal complexes, improved bioavailability, target specificity and therapeutic efficacy in drug design [8-10].

It is widely reported that metal complexes exhibited superior antifungal activity suggesting that coordination with the ligand enhances its effectiveness, possibly by improving membrane penetration or altering its mode of action [11,12]. Conversely, the cytotoxicity assays on MCF-7 breast cancer cells revealed enhanced anticancer activity upon metal complexation, with the metal-ligand complex exhibiting a significantly lower IC_{50} value compared to the free ligand, indicating improved potency following coordination [13,14]. The observed variation in bioactivity highlights the significant influence of metal coordination on the compound's biological behaviour, enhancing certain therapeutic effects while attenuating others. These trends provide valuable insights for the rational design of metallodrugs, particularly in optimizing metal-ligand frameworks for targeted therapeutic applications [15,16]. Moreover, the findings emphasize the importance of comprehensive biological evaluation during the development of coordination compounds with tailored pharmacological profiles and they further underscore the need for in-depth mechanistic studies to elucidate the structural determinants underlying their selective bioactivity [17].

Based on these facts, this study was undertaken to explore the potential of valine-derived ligands in the design of biologically active metal complexes. By synthesizing and charact-

erizing a novel Cd(II) complex of N-[2-hydroxy-3-methyl-benzyl]valine and evaluating its antimicrobial, antioxidant, and anticancer properties through both the experimental and computational (DFT) methods, we aim to contribute to the development of metal-based therapeutic agents.

EXPERIMENTAL

All metal salts were procured from commercial suppliers and employed without further purification. Moreover, Sigma-Aldrich provided the AR-grade reagents, such as *o*-cresol, valine, acetic acid, sodium acetate trihydrate and dimethyl-formamide. The FTIR analysis was performed with the Perkin-Elmer 4100 spectrophotometer within the 4000-400 cm^{-1} range. The ^1H NMR spectra were recorded in DMSO-d_6 using a 400 MHz Brunauer spectrometer. The PXRD data was analyzed using X'pert HighScore Plus and processed with baseline corrections in Origin software.

Synthesis of ligand: The ligand was synthesized by mixing equimolar quantities (0.5 mol each) of *o*-cresol (54 g), valine (58.6 g) and sodium acetate trihydrate (68 g) in 250 mL of formalin and glacial acetic acid. The components were stirred until a homogeneous solution was obtained. Subsequently, 40% of formalin solution was added gradually to the mixture while it was heated in a water bath maintained at 60-80 ºC for 2-3 h. After this initial reaction period, the entire solution was subjected to prolonged heating in a water bath for 12-14 h with intermittent stirring. Upon cooling, a yellowish viscous liquid to waxy solid was formed. This crude product was transferred to distilled water and filtered. A portion of the filtrate was purified by recrystallization using NaOH followed by treatment with 50% HCl (**Scheme-I**). The resulting precipitate was dried in an oven at a controlled temperature of 20-30 ºC for 2-3 days.

Synthesis of metal complex: The equimolar quantities of ligand, N-[2-HMBV-3] (0.237 g, 0.001 mol) and cadmium acetate (0.230 g, 0.001 mol) were each dissolved separately in 10 mL of DMSO and 10 mL of distilled water, respectively, under continuous stirring until clear, homogeneous solutions were obtained. The two solutions were then combined and the resulting mixture was heated in a water bath at 60-80 ºC for 12-14 h to facilitate complexation. Upon completion of the reaction, a solid precipitate was formed, collected, washed thoroughly with distilled water and finally allowed to dry at ambient temperature (20-30 ºC), yielding the anhydrous form of the desired metal complex (**Scheme-II**).

Antimicrobial activities: Amphotericin B was employed as reference standard for evaluating the antifungal efficacy of ligand N-[2-HMBV-3] and its cadmium(II) complex against *Aspergillus niger*. Both compounds were tested at concentrations of 25, 50, 75 and 100 μg/mL. The antibacterial activity against *Escherichia coli* was evaluated at the same concentration range, with ciprofloxacin serving as positive control. The effectiveness of the test samples was quantified by determining their minimum inhibitory concentration (MIC) values, facilitating the comparative analysis.

DPPH radical scavenging assay: The antioxidant potential of the compounds was determined *via* DPPH radical scavenging activity. Briefly, 10 μL of each test sample or the standard antioxidant (ascorbic acid) was added to 0.2 mL of 0.1 mM DPPH solution prepared in methanol, in a 96-well microplate. The assay was performed in quadruplicate including duplicate blanks (DPPH + sample/standard) and controls (DPPH + 20 μL water). After incubating in dark for 30 min at room temperature, absorbance was measured at 517 nm using a BioRad iMark microplate reader. Radical scavenging activity (RSA%) was calculated as:

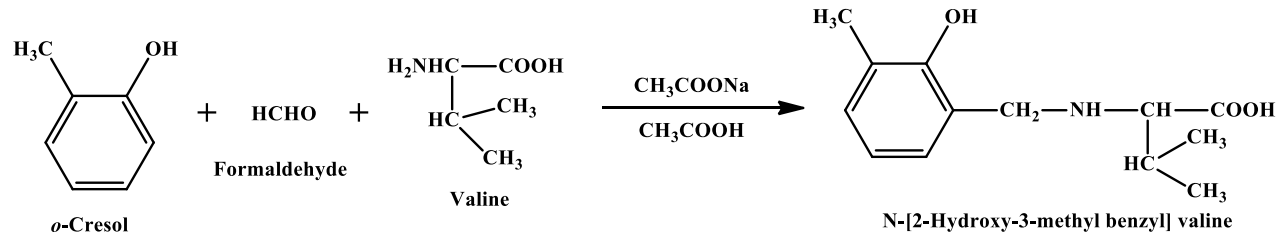

Scheme-I: Synthesis of N-[2-hydroxy-3-methyl-benzyl]valine (ligand)

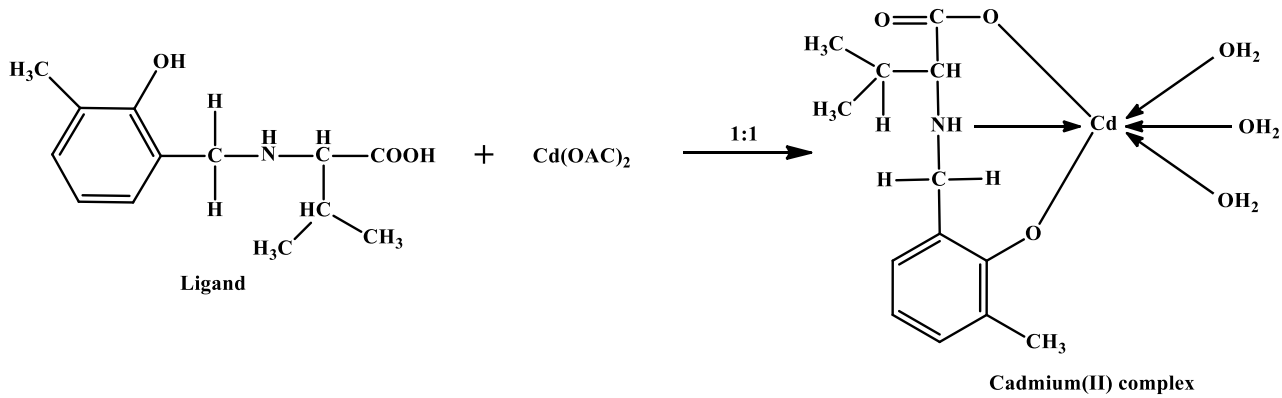

Scheme-II: Synthesis of cadmium(II) complex

$$\text{RSA } (\%) = \frac{\text{Abs}_{\text{control}} - \text{Abs}_{\text{sample}}}{\text{Abs}_{\text{control}}} \times 100$$

Half-maximal inhibitory concentration (IC_{50}) values were derived by plotting concentration (X-axis) against percentage inhibition (Y-axis) using GraphPad Prism 6. The results are reported as mean ± SEM.

Cytotoxicity assay: The cytotoxic effects of the ligand and its Cd(II) complex were evaluated against MCF-7 breast cancer cells using the MTT assay. Cells were seeded at a density of 10,000 cells per well in multi-well plates containing Dulbecco's Modified Eagle Medium (DMEM) supplemented with 10% fetal bovine serum (FBS) and 1% antibiotics, then incubated at 37 ºC in a 5% CO_2 atmosphere for 24 h. Test compounds, prepared in DMSO and diluted in serum-free medium, were applied at varying concentrations, with untreated cells serving as the negative control. Following 24 h of treatment, MTT reagent (5 mg/mL) was added to each well and incubated for 2 h. The resulting formazan crystals were dissolved in DMSO and absorbance was recorded at 540 nm using an iMark ELISA reader. The IC_{50} values were calculated with GraphPad Prism 6 and the cellular morphology changes were captured using inverted microscopy (Olympus EK2) equipped with an AmScope camera. Data are expressed as mean ± SEM, with IC_{50} representing the concentration required to reduce cell viability by 50%.

RESULTS AND DISCUSSION

FTIR spectral studies: FT-IR analysis of N-[2-hydroxy-3-methylbenzyl]valine (2-HMBV-3) and its cadmium(II) complex provides valuable insights into their structural features and coordination behaviour. The free ligand shows a wide O-H stretching vibration of the phenolic -OH group between 3600 and 3200 cm^{-1}, which shows that there is a hydroxyl group attached to the aromatic ring [18]. Aromatic C-H stretching vibrations appears in the 3100-3000 cm^{-1} range, while the stretching from the methyl group's alkyl C-H appears at 2960 -2850 cm^{-1}. The secondary amine group exhibits the N-H stretching at 3500-3300 cm^{-1} and N-H bending at 1600-1500 cm^{-1} [19]. The carboxylic acid group has a wide O-H stretching band (2500-3300 cm^{-1}) due to hydrogen bonding and a strong C=O stretching peak at 1750-1700 cm^{-1} from the carbonyl bond [20] (Fig. 1).

Complexation with cadmium(II) ions causes large shifts in the IR peaks, indicating the ligand-metal coordination. The carboxylate group exhibits two distinct C=O stretching vibrations *viz*. an asymmetric stretch appearing between 1650 and 1600 cm^{-1}, and a symmetric stretch observed within the 1450-1350 cm^{-1} range, both of which signify the coordination to the cadmium ion. The amide group shows the N-H stretching between 3500-3200 cm^{-1} and C=O stretching from 1690-1650 cm^{-1}, which confirmed that the amide carbonyl is coordinated to the metal. Aromatic C-H stretching occurs between 3100-3000 cm^{-1}, while the C=C stretching in the aromatic ring is appeared at 1600-1450 cm^{-1}. The presence of coordinated water molecules is supported by significant O-H stretching at 3500-3300 cm^{-1} and H-O-H bending at 1640-1600 cm^{-1} [19]. Moreover, the stretching vibrations of metal-oxygen (Cd-O)

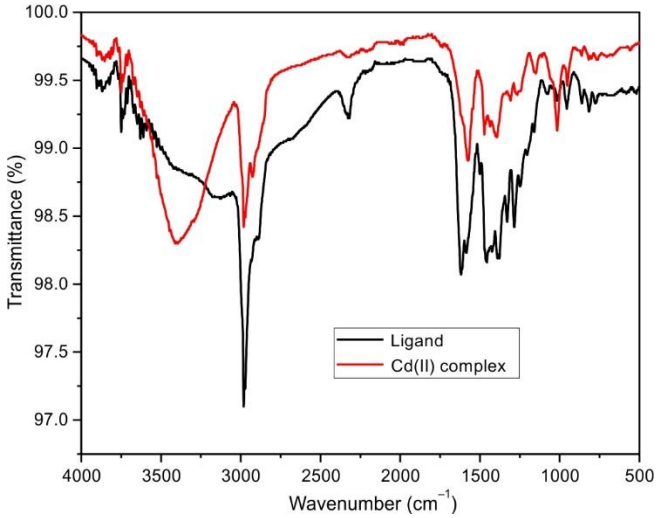

Fig. 1. FT-IR spectra of ligand and its Cd(II) metal

are appeared in the 600-400 cm^{-1} range, whereas the stretching of metal-nitrogen (Cd-N) appears at 550-450 cm^{-1}, which confirmed that cadmium is bonded to oxygen and nitrogen atoms from the ligand (Fig. 1). The spectral shifts confirmed the formation of the cadmium complex, coordinated with the ligand's carboxylate, amide and potentially amine groups.

NMR spectral studies: The ^{1}H NMR spectrum of ligand *N*-[2-hydroxy-3-methylbenzyl]valine, recorded in DMSO-d_6 on a 400 MHz spectrometer, exhibits signals consistent with the expected proton environments. The phenolic –OH proton resonates at δ 9.67 ppm as a deshielded singlet due to the intramolecular hydrogen bonding and the electronegative oxygen atom, while the amide –NH proton of the valine moiety appears at δ 8.83 ppm, reflecting deshielding from the adjacent carbonyl group [21]. Aromatic protons on the 1,2,3-trisubstituted benzene ring appear as multiplets between δ 7.18 and 6.99 ppm. The benzylic –CH_2– group attached to the nitrogen and aromatic ring resonates at δ 4.98 ppm, slightly deshielded by the electron-withdrawing effects of both the aromatic ring and nitrogen [22]. The α-proton of valine appears at δ 3.92 ppm, with the neighbouring methylene protons at δ 3.52 ppm. The methyl group on the aromatic ring resonates at δ 2.62 ppm, while the β-methylene protons of the valine side chain appear at δ 2.20 and 2.13 ppm. The isopropyl methyl groups of valine are observed as doublets at δ 1.03 and 0.96 ppm. Upon complexation with Cd(II), the phenolic –OH proton is either significantly shifted or disappears, indicating deprotonation and coordination to the metal center, while the amide –NH and other aliphatic protons experience minor downfield shifts due to changes in the electronic environment. These observations suggest that Cd(II) coordinates through both the phenolic oxygen and the amide nitrogen, forming a stable chelate, likely adopting a distorted octahedral or tetrahedral geometry, with the aromatic ring and hydroxyl group enhancing the overall stability through electron donation [23].

^{13}C NMR spectral studies: The comparison of the ^{13}C NMR spectra of free ligand and its metal complex reveals the significant chemical shift changes, confirming coordination to the metal center. In the free ligand, the carboxylate carbonyl resonates at δ 174.96 ppm, characteristic of the protonated

carboxylic acid group, whereas upon complexation, this signal shifts downfield to δ 178-185 ppm due to the deprotonation and direct coordination to the metal, reflecting reduced electron density at the carbon [24]. The aromatic carbon bearing the hydroxyl group undergoes a notable shift from δ 151.43 ppm in the free ligand to δ 140-145 ppm in the complex, consistent with deprotonation of the phenolic –OH and coordination to the metal center. Other aromatic carbons (δ 136.03-113.81 ppm) show minor shifts and slight broadening, indicating subtle redistribution of π-electron density upon complexation. The benzylic carbon, initially at δ 65.81 ppm, may shift to higher ppm values due to its proximity to the coordination site. The α- and β-carbons of valine (δ 48.63 and 39.96 ppm, respectively) exhibit minor changes, particularly if the amino nitrogen participates in metal binding. The methyl carbons (δ 28.26, 18.54 and 17.17 ppm) generally remain unaffected, except when near the metal coordination sphere [25]. Collectively, these ^{13}C NMR variations provide clear evidence for complex formation, with the most pronounced changes observed at the carboxylate and phenolic carbons, indicating that these atoms serve as the primary binding sites for the metal center.

UV-Vis spectral studies: The UV-Vis spectral study of valine derivative and its Cd(II) complex reveals the distinct electronic transitions and metal-ligand interactions. The free ligand exhibits the absorption peaks at 294.69, 352.02 and 520.14 nm, corresponding to π-π* and n→π* transitions, reflecting the conjugation effects [26]. Upon coordination with Cd(II), these peaks shift to 280.39, 342.44 and 569.98 nm, indicating the formation of a metal-ligand complex. The appearance of the 569.98 nm peak suggests a metal-to-ligand charge transfer (MLCT) transition. The shifts in the spectra, including a hypsochromic shift for π-π* transitions and a bathochromic shift for MLCT, confirm coordination of Cd(II) through the -NH, -COO and -OH donor groups (Fig. 2) [27].

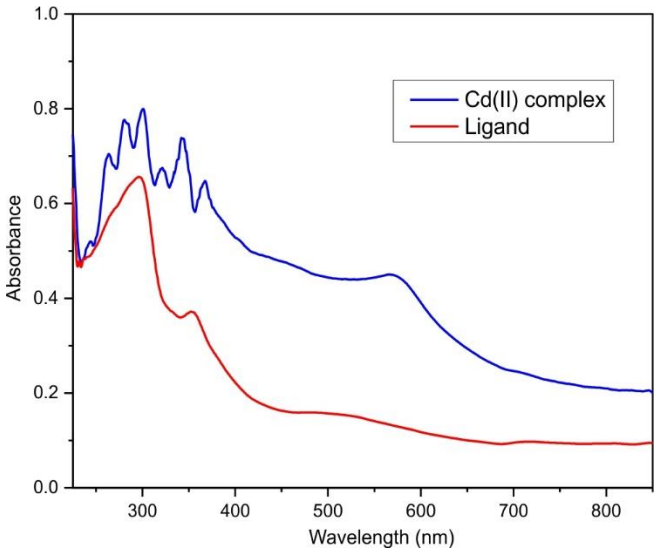

Fig. 2. UV-vis spectra of ligand and its Cd(II) metal

Powder XRD: The PXRD analysis further elucidates the crystalline structures of the ligand and its metal complex. The ligand crystallizes in a monoclinic system (space group $P2_1/a$) with unit cell dimensions a = 5.2260 Å, b = 11.5740 Å, c = 3.9628 Å, and angles α = 90º, β = 120º, γ = 90º, giving a unit cell volume of 237.54 × 10^6 pm^3. In contrast, the Cd(II) complex adopts a hexagonal crystal system (space group $P6_3/mmc$) with a = b = 2.9793 Å, c = 5.6181 Å, α = β = 90º, γ = 120º and a reduced unit cell volume of 43.19 × 10^6 pm^3, suggesting denser packing and higher crystallinity, as reflected in its higher density of 8.64 g/cm^3 compared to 1.60 g/cm^3 for the ligand [28,29]. The hexagonal system features symmetry elements such as a six-fold screw axis, mirror planes, and glide planes, which influence the PXRD peak positions and intensities (Fig. 3). The average crystallite size of the metal complex calculated using the Debye-Scherrer equation ($D = 0.9\lambda/\beta\cos\theta$) with λ = 1.54 Å, β as the full width at half maximum (FWHM), and θ the Bragg angle), was determined to be 25.5 nm (Table-1). The number of formula units per unit cell (Z) was also calculated using the equation $Z = \rho V N_A/M$, where ρ denotes the density; V represents the unit cell volume; N_A stands for Avogadro's number; and M is the molar mass.

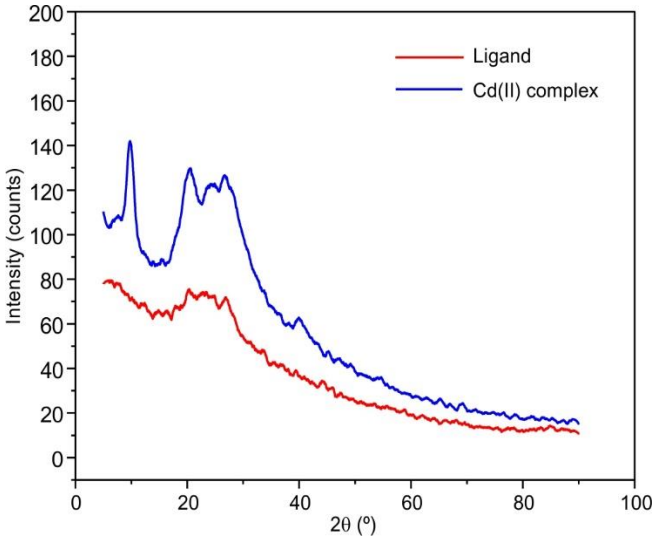

Fig. 3. PXRD spectra of ligand and its Cd(II) metal

TABLE-1
CRYSTALLOGRAPHIC DATA

	Ligand	Metal complex
Temperature (K)	298	298
Wavelength (Å)	1.54	1.54
Crystal system	Monoclinic	Hexagonal
Space group	$P2_1/a$	$P6_3/mmc$
Unit cell dimensions	a = 5.2260 Å b = 11.5740 Å c = 3.9628 Å α = γ = 90º, β = 120º	a = 2.9793 Å b = 2.9793 Å c = 5.6181 Å α = β = 90º, γ = 120º
Volume (10^6 pm^3)	237.54	43.19
2θ range	0-90º	0-90º
Limiting indices	$0 \le h \le 3$, $0 \le k \le 1$, $0 \le l \le 6$	$0 \le h \le 3$, $0 \le k \le 6$, $0 \le l \le 2$
Density (g/cm^3)	1.60	8.64
Z	2.00	2.00
CCDC number	00-036-1684	00-005-0674

SEM studies: The SEM examination provided significant insights into the morphological and structural differences bet-

ween *N*-[2-hydroxy-3-methylbenzyl]valine and its cadmium(II) complex. The free ligand exhibited agglomerated, irregularly shaped particles with a porous and rough texture, indicative of non-uniform crystallinity and weak intermolecular interactions (Fig. 4a) [30]. In contrast, upon complexation with cadmium, significant morphological changes were observed. The Cd(II) complex displayed a more compact, tightly packed structure with increased homogeneity and grain size, suggesting enhanced molecular stability. Surface smoothness improved due to stronger coordination bonds between cadmium and the donor groups (-NH, -COO, -OH), while surface roughness decreased, confirming effective metal-ligand interaction (Fig. 4b) [31,32]. The SEM results therefore validate the successful formation of the cadmium complex and the structural stabilization.

DFT studies: DFT optimization at the B3LYP/6-31G level showed that coordination of Cd^{2+} with the ligand induces significant structural and electronic changes. Formation of Cd–O (4.125-6.004 Å) and Cd–N (5.750 Å) bonds confirms metal-ligand interaction, with elongation of key bonds such as C12–O20 (2.042 Å) and N23–C12 (1.763 Å) indicating the electron density redistribution. The initially planar ligand distorts to accommodate a distorted octahedral geometry, evidenced by unusual bond angles (O18–Cd24–O22 = 140.27º, O20–Cd24–O21 = 45.02º), highlighting the participation of carbonyl and amine groups in coordination (Fig. 5, Table-2). These theoretical findings are consistent with experimental observations, confirming the reliability of DFT in predicting the coordination-induced structural changes.

Antimicrobial activities: The antifungal activity against *A. niger* was measured through percentage inhibition at various concentrations for the ligand, Cd(II) complex and amphotericin B as reference. Amphotericin B showed the highest inhibition across all the concentrations. While the cadmium(II) complex generally exhibited stronger antifungal activity than the free ligand, showing a concentration-dependent effect (Fig. 6a). Antibacterial activity against *E. coli* was similarly tested using ciprofloxacin as a standard. Ciprofloxacin consistently demonstrated the highest inhibition, while the ligand exhibited greater antibacterial activity than the cadmium(II) complex at most concentrations (Fig. 6b). MIC values confirmed that the ligand was more potent than the complex against both *E. coli* and *A. niger*, whereas standard drugs showed superior efficacy.

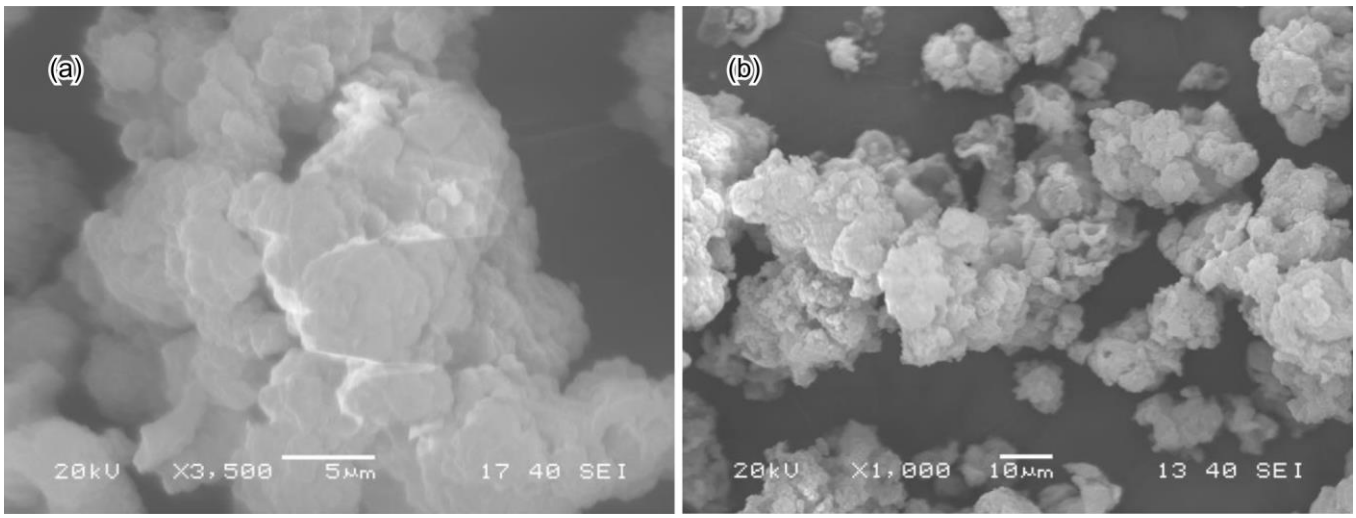

Fig. 4. SEM images of (a) ligand and (b) its Cd(II) complex

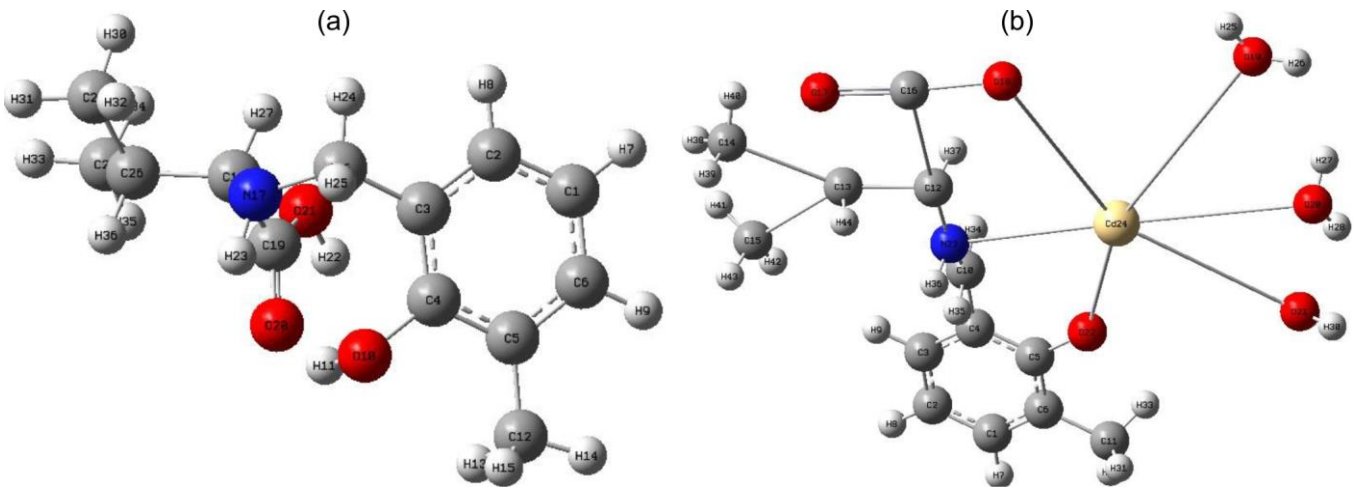

Fig. 5. Optimized structures of (a) ligand and (b) its Cd(II) complex

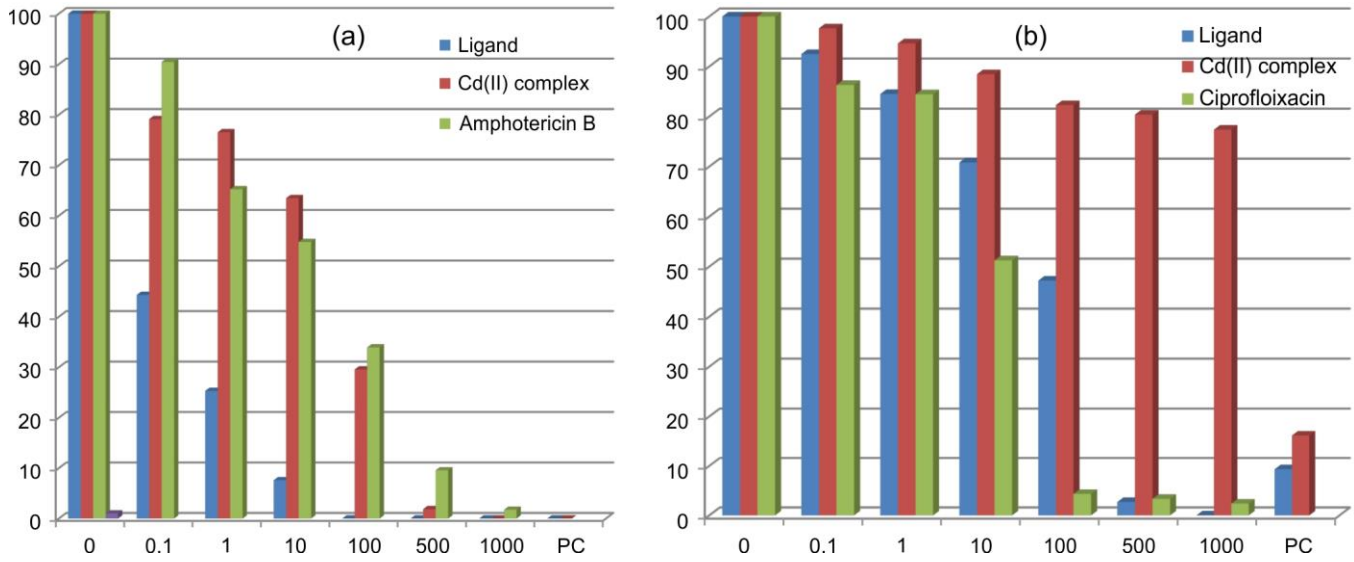

Fig. 6. (a) *A. niger* (antifungal) and (b) *E. coli* (antibacterial) properties of ligand and its Cd(II) complex

TABLE-2
BOND LENGTH AND BOND ANGLES OF
OPTIMIZED LIGAND AND ITS Cd(II) COMPLEX

Bond	Bond length (Å)	Bond	Bond angle (°)
Ligand			
C16-N17	1.471	C16-N17-C18	119.915
N17-C18	1.457	C3-C4-O10	119.539
C18-C19	1.525	C19-O21-O20	62.681
C18-C26	1.568	C26-C28-C29	110.989
C26-C29	1.538	N17-C16-C3	118.713
C26-C28	1.541	C1-C2-C3	120.886
C19-O20	1.245	C4-C5-C6	118.164
C3-C16	1.526	C4-C5-C12	120.012
C4-O10	1.410		
C5-C12	1.509		
C1-C2	1.397		
C2-C3	1.404		
C3-C4	1.403		
C4-C5	1.407		
Cadmium(II) complex			
C12-H37	1.07000	O21-Cd24-O19	95.15476
N23-H36	1.00000	O20-Cd24-O19	50.13417
C4-O5	1.39482	O20-Cd24-O21	45.02060
C5-O22	1.43000	O18-Cd24-O22	140.26936
C4- O10	1.54000	O18-Cd21-O20	54.46603
C10-N23	1.56251	O22-Cd24-N23	63.79209
N23-C12	1.76308	O18-Cd24-N23	
O18- C16	2.00236		
C16-O17	1.89113		
Cd24-O18	4.90449		
N23-Cd24	3.602025		

Antioxidant activity: DPPH radical scavenging activity revealed significant differences between ascorbic acid, ligand and its cadmium(II) complex at concentrations ranging from 0-1000 μM. At low concentrations (1-10 μM), the ligand showed superior activity (5.89-6.59 nm) compared to the it's Cd(II) complex (2.89–6.34 nm) and ascorbic acid (0.69-4.94 nm). At higher concentrations, ascorbic acid exhibited stronger activity, reaching 1416.20 nm at 1000 μM, while the Cd(II) complex (1349.47 nm) surpassed the ligand (1279.45 nm) (Fig. 7). Metal coordination enhances radical stabilization through electron delocalization, suggesting that the cadmium complex could serve as an effective alternative antioxidant, particularly at higher concentrations [33].

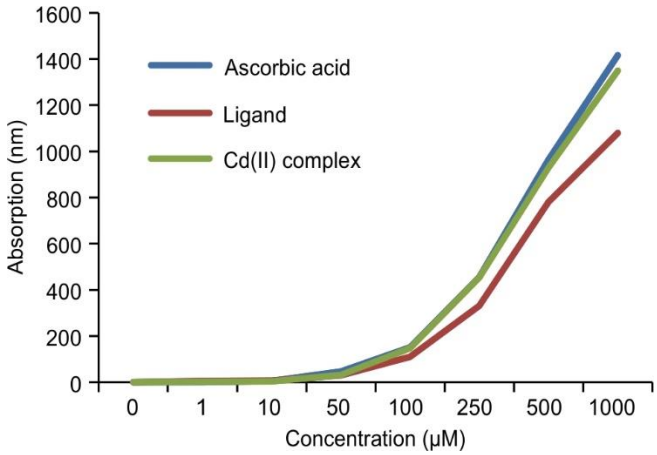

Fig. 7. Antioxidant properties of ligand and its Cd(II) complex

Anticancer activity: The MTT assay on MCF-7 cells showed that paclitaxel was the most potent (IC_{50} = 125.1 ± 0.20 nM), consistent with its microtubule-stabilizing effect [34]. The cadmium complex (IC_{50} = 550.5 ± 0.19 μM) was approximately 4.4 times more cytotoxic than the free ligand (IC_{50} = 633 ± 0.07 μM), although both were significantly less potent than paclitaxel. The enhanced activity of the Cd(II) complex may result from the metal's contribution to cellular uptake or redox activity, and both compounds showed dose-dependent cytotoxicity, particularly at 100-1000 nM (Fig. 8). These results indicate that metal complexation substantially improves the anticancer potential of the valine-derived ligand.

Conclusion

In this work, a novel cadmium(II) complex of N-[2-hydroxy-3-methylbenzyl]valine was successfully synthesized

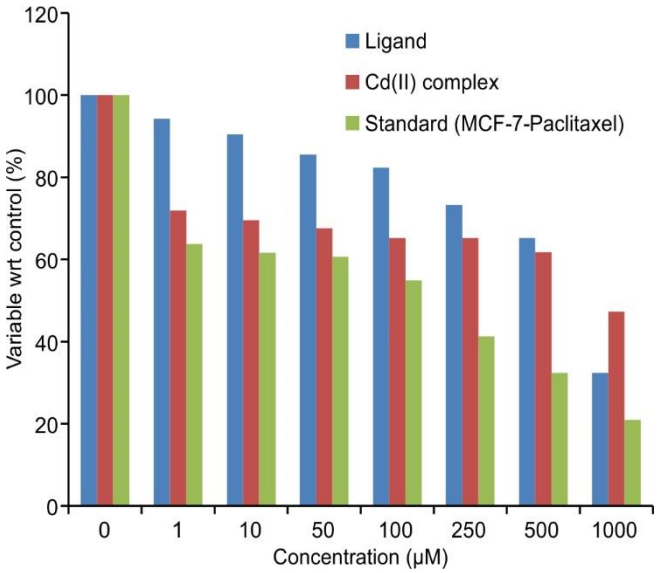

Fig. 8. Anticancer properties of ligand and its Cd(II) complex

and characterized using a combination of experimental (FTIR, NMR, UV-Vis, PXRD, SEM) and computational (DFT) techniques. Spectroscopic analyses confirmed the coordination of cadmium through the carboxylate, amide and phenolic groups present in ligand, leading to significant structural and electronic changes. PXRD and SEM studies revealed a transformation from a monoclinic ligand structure to a hexagonal, densely packed and stable metal complex. DFT calculations supported the experimental findings, indicating a distorted octahedral geometry and redistribution of electron density upon complexation. Biological evaluation demonstrated that Cd(II) complex enhanced certain activities while diminishing others. The Cd(II) complex exhibited superior antifungal activity against *A. niger* and stronger anticancer activity against MCF-7 breast cancer cells compared to the free ligand. Conversely, the ligand displayed greater antibacterial activity against *E. coli* and higher antioxidant activity at lower concentrations. These results underscore the influence of metal coordination on the pharmacological profile of the ligand, highlighting the potential of valine derived Cd(II) complexes as therapeutic agents with selective bioactivity.

ACKNOWLEDGEMENTS

One of the authors, Dr. Gugulothu Vinod, gratefully acknowledges the financial support received from Council of Scientific & Industrial Research (CSIR-HRDG), Government of India, New Delhi, India (Ref. no. 09/132(0879)/2018 EMR-I).

CONFLICT OF INTEREST

The authors declare that there is no conflict of interests regarding the publication of this article.

REFERENCES

1. S. Wu, M. Wang, Z. Liu and C. Fu, *Microorganisms*, **13**, 1570 (2025); https://doi.org/10.3390/microorganisms13071570
2. S. Kothandan and A. Sheela, *Mini-Rev. Med. Chem.*, **21**, 1909 (2021); https://doi.org/10.2174/1389557521666210308143522
3. F. Arjmand and A. Jamsheera, *Spectrochim. Acta A: Mol. Biomol. Spectrosc*., **78**, 45 (2011); https://doi.org/10.1016/j.saa.2010.06.009
4. A.M. Nijasure, V.N. Joshi and A.D. Sawant, *J. Inorg. Biochem*., **73**, 109 (1999); https://doi.org/10.1016/S0162-0134(99)00008-2
5. F. Mohammadi, H. Mansouri-Torshizi, M. Saeidifar, E. Dehghanian, E. Skorepova, M. Dusek and K. Abdi, *Nucleosides Nucleotides Nucleic Acids*, **41**, 97 (2022); https://doi.org/10.1080/15257770.2021.2011914
6. Z. Vargová, P. Olejníková, G. Kuzderová, M. Rendošová, J. Havlíčková, R. Gyepes and M. Vilková, *Bioorg. Chem.*, **141**, 106907 (2023); https://doi.org/10.1016/j.bioorg.2023.106907
7. G. Sasikumar, A. Subramani, R. Tamilarasan, P. Rajesh, P. Sasikumar, S. Albukhaty, M.K.A. Mohammed, S. Karthikeyan, Z.T. Al-Aqbi, F. A.J. Al-Doghachi and Y.H. Taufiq-Yap, *Molecules*, **8**, 2931 (2023); https://doi.org/10.3390/molecules28072931
8. S. Thota, D.A. Rodrigues, D.C. Crans and E.J. Barreiro, *J. Med. Chem*., **61**, 5805 (2018); https://doi.org/10.1021/acs.jmedchem.7b01689
9. J. Lv, T. Liu, S. Cai, X. Wang, L. Liu and Y. Wang, *J. Inorg. Biochem.*, **100**, 1888 (2006); https://doi.org/10.1016/j.jinorgbio.2006.07.014
10. W. K. Kim, J. M. An, Y. J. Lim, K. Kim, Y. H. Kim and D. Kim, *Mater. Today Adv*., **25**, 100569 (2025); https://doi.org/10.1016/j.mtadv.2025.100569
11. O.A. Dar, S.A. Lone, M.A. Malik, M.Y. Wani, M.I.A. Talukdar, A S. Al-Bogami, A.A. Hashmi and A. Ahmad, *Appl. Organomet. Chem.*, **33**, e5128 (2019); https://doi.org/10.1002/aoc.5128
12. A. Frei, A.G. Elliott, A. Kan, H. Dinh, S. Bräse, A.E. Bruce, M.R. Bruce, F. Chen, D. Humaidy, N. Jung, A.P. King, P.G. Lye, H.K. Maliszewska, A.M. Mansour, D. Matiadis, M.P. Muñoz, T.-Y. Pai, S. Pokhrel, P.J. Sadler, M. Sagnou, M. Taylor, J.J. Wilson, D. Woods, J. Zuegg, W. Meyer, A.K. Cain, M.A. Cooper and M.A.T. Blaskovich, *JACS Au*, **2**, 2277 (2022); https://doi.org/10.1021/jacsau.2c00308
13. I. Waziri, S. Sookai, T.L. Yusuf, K.A. Olofinsan and A.J. Muller, *Appl. Organomet. Chem.*, **39**, e70162 (2025); https://doi.org/10.1002/aoc.70162
14. S. Abdolmaleki, S. Khaksar, A. Aliabadi, A. Panjehpour, E. Motieiyan, D. Marabello, M. H. Faraji and M. Beihaghi, *Toxicology*, **492**, 153516 (2023); https://doi.org/10.1016/j.tox.2023.153516
15. S. Adhikari, P. Nath, A. Das, A. Datta, N. Baildya, A.K. Duttaroy and S. Pathak, *Biomed. Pharmacother*., **171**, 116211 (2024); https://doi.org/10.1016/j.biopha.2024.116211
16. H. Y. Khan, M. F. Ansari, S. Tabassum, and F. Arjmand, *Drug Discov. Today*, **29**, 104055 (2024); https://doi.org/10.1016/j.drudis.2024.104055
17. P.E. Marinova and K.D. Tamahkyarova, *Compounds*, **5**, 14 (2025); https://doi.org/10.3390/compounds5020014
18. M.S.A. Mansour, A.T. Abdelkarim, A.A. El-Sherif and W.H. Mahmoud, *BMC Chem*., **18** 150 (2024); https://doi.org/10.1186/s13065-024-01239-7
19. J. Dong, L. Li, G. Liu, T. Xu, and D. Wang, *J. Mol. Struct*., **986**, 57 (2011); https://doi.org/10.1016/j.molstruc.2010.11.036
20. M.M. Salama, S.G. Ahmed and S.S. Hassan, *Adv. Biol. Chem*., **7**, 182 (2017); https://doi.org/10.4236/abc.2017.75013
21. D. Dinku, T.B. Demissie, I.N. Beas and T. Desalegn, *Results Chem.*, **8**, 101562 (2024); https://doi.org/10.1016/j.rechem.2024.101562
22. V. Tugarinov, V. Venditti, and G. M. Clore, *J. Biomol. NMR*, **58**, 1 (2013); https://doi.org/10.1007/s10858-013-9803-1
23. J. Lv, T. Liu, S. Cai, X. Wang, L. Liu and Y. Wang, *J. Inorg. Biochem.*, **100**, 1888 (2006); https://doi.org/10.1016/j.jinorgbio.2006.07.014
24. H.L. Singh, *Main Group Metal Chem.*, **39**, 67 (2016); https://doi.org/10.1515/mgmc-2015-0039

25. M.A. Ashraf, A. Wajid, K. Mahmood, M.J. Maah and I. Yusoff, *Orient. J. Chem.*, **27**, 260 (2011).
26. S. Mandal, G. Das and H. Askari, *RSC Adv.*, **4**, 24796 (2014); https://doi.org/10.1039/C4RA01288G
27. S. Musa, S.O. Idris, D.A. Onu and A.B. Suleiman, *Avicenna J. Environ. Health Eng.*, **6**, 100 (2019); https://doi.org/10.34172/ajehe.2019.13
28. E. López-Torres and M. A. Mendiola, *Polyhedron*, **24**, 1435 (2005); https://doi.org/10.1016/j.poly.2005.03.093
29. K.A. Dahlous, A.A.M. Alotaibi, N. Dege, A. El-Faham, S.M. Soliman and H.M. Refaat, *Crystals*, **12**, 861 (2022); https://doi.org/10.3390/cryst12060861
30. M.I. Khan, A. Khan, I. Hussain, M.A. Khan, S. Gul, M. Iqbal, I.-U. Rahman and F. Khuda, *Inorg. Chem. Commun.*, **35**, 104 (2013); https://doi.org/10.1016/j.inoche.2013.06.014
31. N. Sridevi and D. Madheswari, *Polyhedron*, **282**, 117796 (2025); https://doi.org/10.1016/j.poly.2025.117796
32. W.H. Mahmoud, R.G. Deghadi and G.G. Mohamed, *Appl. Organomet. Chem.*, **32**, e4289 (2018); https://doi.org/10.1002/aoc.4289
33. Z. Chen, R. Świsłocka, R. Choińska, K. Marszałek, A. Dąbrowska, W. Lewandowski and H. Lewandowska, *Int. J. Mol. Sci.*, **25**, 11775 (2024); https://doi.org/10.3390/ijms252111775
34. M. Armat, T.O. Bakhshaiesh, M. Sabzichi, D. Shanehbandi, S. Sharifi, O. Molavi, J. Mohammadian, M.S. Hejazi and N. Samadi, *Bosn. J. Basic Med. Sci.*, **16**, 28 (2016); https://doi.org/10.17305/bjbms.2016.674